## **JQS**

## **Journal of Quaternary Science**



# Radiocarbon and stable isotope evidence of early to mid-Holocene wet events from fluvial tufa deposits in Santa Cruz, CA

MAURA C. KANNER, 1\* D LUIS CORTES and YADIRA IBARRA 1\* D

<sup>1</sup>Earth and Climate Sciences Department, San Francisco State University, San Francisco, California, 94132, USA <sup>2</sup>Earth and Planetary Sciences Department, University of California, Santa Cruz, Santa Cruz, California, 95064, USA

Received 13 January 2022; Revised 30 May 2022; Accepted 1 June 2022

ABSTRACT: It is increasingly important to document past records of hydrologic change in areas that are drought-prone to better predict the region's future vulnerability to recharge and water supply. Holocene spring-associated carbonate deposits serve as terrestrial records of water balance that can complement other local, high-resolution proxies that are moisture-sensitive. Here we examine two carbonate deposits (one inactive perched tufa site and one active fluvial tufa site) that form from ambient-temperature freshwater springs, as proxies of their depositional conditions. Radiocarbon ( $^{14}$ C) analyses of charcoal fragments from the inactive perched tufa record depositional ages of  $6.2 \pm 0.06$  ( $2\sigma$ ) cal ka BP and  $8.0 \pm 0.04$  ( $2\sigma$ ) cal ka BP and agree with the age models from other proxies of past pluvial periods in the region ( $\sim$ 16 to 5 ka). The active fluvial tufas date to  $853 \pm 0.4$  cal BP, representing conditions similar to modern flow. Geomorphologic and radiocarbon results indicate the perched tufa reflects wetter conditions fed by a higher water table. Stable isotopic analyses of carbonate ( $\delta^{13}$ C,  $\delta^{18}$ O) reveal distinct isotopic values between modern and early-mid-Holocene tufa. This work underscores potential for the analysis of other moisture-sensitive tufa deposits in coastal central California. © 2022 John Wiley & Sons, Ltd.

KEYWORDS: stable isotopes; mid-Holocene; pluvial; radiocarbon; tufa

#### Introduction

The central California coast experiences interannual variability in precipitation, with shifts in hydroclimate that lead to widespread drought and reduced water availability (Cook et al., 2015). In the coming decades, climate change is projected to reduce water availability in dryland regions worldwide (Jasechko and Perrone, 2021; Yao et al., 2020) and the already water-stressed desert regions of the southwestern United States (Cook et al., 2015; Seager et al., 2014). California's climate is also expected to become more variable with more projected dry and wet extremes (Swain et al., 2018). These concerns have motivated improved understanding of the impact of drying and wetting on groundwater processes throughout the Quaternary as a means to predict the future of water availability in California. Research across the western United States has resulted in a variety of terrestrial records that encode Quaternary changes in hydrologic balance (Knott et al., 2018; Springer et al., 2015).

Tufa deposits are terrestrial carbonates that form from ambient-temperature spring water (Ford and Pedley, 1996) and can serve as potential archives of palaeoclimate (Andrews, 2006). The presence of metre-scale ancient tufa accumulations in semi-arid regions is indicative of past episodes of greater groundwater recharge, or past pluvials (Capezzuoli *et al.*, 2014; Ibarra *et al.*, 2015; Viles *et al.*, 2007). Distinct facies and erosional features can be indicative of historical changes in water discharge (Arenas *et al.*, 2014a,b; Viles *et al.*, 2007; Capezzuoli *et al.*, 2014).

Understanding these past changes in hydroclimate can provide context for how the region's hydroclimate will vary in the future. Santa Cruz, California hosts several tufa deposits that remain unexplored with respect to their palaeohydroclimatic significance

(e.g. Ibarra and Sanon, 2019). Tufa investigations from similar climates at comparable latitudes around the world have been shown to record Quaternary episodes of wet events (e.g. Andrews et al., 2000; Andrews and Brasier, 2005; Arenas et al., 2014b; Arp et al., 2001; Beverly et al., 2015; Cremaschi et al., 2010; Desouky et al., 2015; Ibarra et al., 2015; Kano et al., 2003; Özkul et al., 2013; Pedley, 2009; Rodríguez-Berriguete and Alonso-Zarza, 2019; Sancho et al., 2015; Sanders et al., 2010; Viles et al., 2007), thus highlighting their promise as terrestrial hydroclimate archives.

The formation of spring-associated tufa is commonly associated with regions that have a limestone, metamorphic and/or volcanic component to the bedrock, under a range of seasonal environmental conditions (Arenas et al., 2014a,b; Kano et al., 2003; Matsuoka et al., 2001; Andrews and Brasier, 2005; Rodríguez-Berriguete and Alonso-Zarza, 2019). The principal environmental controls on tufa deposition include water temperature, stream velocity, water chemistry, water depth, distance from the spring input, and physiological activity of flora and bacteria (Arenas et al., 2014a; Arenas et al., 2014b; Kano et al., 2003; Matsuoka et al., 2001; Andrews and Brasier, 2005). The confluence of these factors, along with regional topography (Viles et al., 2007), control the depositional trends and morphology of tufa deposits (Arenas et al., 2014a; Shiraishi et al., 2010). Seasonal tufa deposition can be represented by millimetre-scale laminae, which can vary in texture, thickness and colour (Arenas et al., 2014a; Arenas and Jones, 2017; Shiraishi et al., 2010). The temperature of cold springs usually mimics the temporal pattern of the air temperature across seasons (Shiraishi et al., 2008). Spring water temperature and pCO<sub>2</sub> can be reflective of the climate and seasonal patterns of the region during tufa formation (Arp et al., 2001; Matsuoka et al., 2001), which can contribute to the type of organisms that thrive in the aqueous spring environment. Spring velocity and turbulence impacts the rate at which tufa can form - high flow velocities and turbulence

\*Corresponding: Maura C. Kanner and Yadira Ibarra, as above Email: mkanner@mail.sfsu.edu and yibarra@sfsu.edu

induces CO<sub>2</sub> degassing from the water, which favours calcite precipitation (Arenas *et al.*, 2014a). Photosynthesis by aquatic microorganisms also impacts tufa formation; however, its exact effect is currently disputed (Shiraishi *et al.* 2008, 2010; Arenas *et al.* 2014a; Spiro and Pentecost, 1991; Andrews and Brasier, 2005).

The analysis of ancient tufa deposits at different spatial scales can reveal depositional information about hydroclimatic conditions, as well as relatively short-lived climatic events (Andrews, 2006; Arenas and Jones, 2017). Although highresolution chronology of ancient tufa deposits is rarely achieved, specific tufa morphologies such as perched spring lines (sensu Pedley et al., 2003), are geomorphologic evidence of water availability and elevated water tables (Domínguez-Villar et al., 2011). This study investigates previously undescribed tufa deposits from Santa Cruz, CA, located in Henry Cowell State Park (Fig. 1). The aims of these analyses are to: (1) constrain the timing of deposition of the ancient tufa mounds; and (2) describe the environment in which the tufa formed. Results from this research will help inform models of future and past changes in hydroclimate in a region projected to experience continued drying under the influence of anthropogenic climate change (Cook et al., 2010).

#### **Environmental setting**

Henry Cowell State Park is located approximately 11 kilometers north of the city of Santa Cruz, CA (Fig. 1). Geologically, the southern part of the park contains schist and granite, while the northern part consists of sandstone and mudstone as well as quartz diorite (Brabb, 1989; California State Parks, 2011). The park is part of the greater Santa Cruz Mountains, and is located between the San Andreas Fault (to the east) and the San Gregorio and Sur-Nacimiento Faults (to the west) (Brabb, 1989). The park is divided into two units, Henry Cowell Redwoods State Park and the Fall Creek Unit (Fig. 1B). Our research site is located in the Fall Creek Unit (Fig. 1B), which encompasses 9.7 km<sup>2</sup> of land as well as the entire Fall Creek watershed (California State Parks, 2011). We investigated an inactive, perched tufa mound as well as an active fluvial tufa channel along Ringtail Creek (Fig. 1C). The fluvial and perched carbonate (tufa) deposits are on Mesozoic or Palaeozoic pelitic schist and quartzite, part of the Salinian block (Brabb, 1989). Ringtail Creek, the water source of interest in this investigation, is one of several streams in the Fall Creek watershed and extends for 1.26 km (Fig. 1C). Water

temperature and pH were measured at the spring source during summer and winter of 2020 (Table 1).

Santa Cruz, CA, has a Mediterranean climate that is characterised by dry summers and cold, wet winters. Precipitation occurs as rain during winter and early spring, and as fog cover in the summer months. Winter storms originate in the mid- to northern Pacific as well as occasional tropical Pacific storms known as atmospheric rivers. This climate is conducive to redwood forests which dominate in the catchment of Ringtail Creek (Fig. 2A). The air temperature is moderate year round, where the average annual high temperature is 22.8°C and the average annual low temperature is 3.9°C (Adam *et al.*, 1981). The average annual precipitation in Felton, CA, is 840 mm (U.S. Department of Commerce, National Climatic Data Center, 2022).

#### Methods

#### Sample collection

Tufa facies were mapped and photodocumented at the outcrop scale. The inactive perched tufa mound in Henry Cowell State Park is approximately 4 m thick and spans a length of approximately 4.5 m (Fig. 2). The perched mound is elevated ~50 m above the valley channel and occurs approximately 15 m south of the current path of Ringtail Creek (Fig. 1C). The steep topography of the area, along with the vegetation and topsoil that sits above the mound, makes it difficult to determine its full extent and macrofacies (e.g. stepped terraces). The mound is wedged into the side of a steep slope and its southern unit resembles waterfall facies with small curtain-like features towards its base (*sensu* Pedley *et al.*, 2003) (Fig. 2B–C). The southern part of the mound that was accessible for sample collection displays drippy speleothems (Fig. 3A–B). One 25 cm long (3 cm diameter) core and three hand samples were

**Table 1.** Water temperature and pH measurements from the source and distalmost pool of the spring (Ringtail Creek) that feeds the fluvial facies.

	) рН
Distal 14 Jan 2020 376 10.4 8.5 Source 9 Jul 2020 472 12.8 7.5	7.29 8.31 7.79 8.29

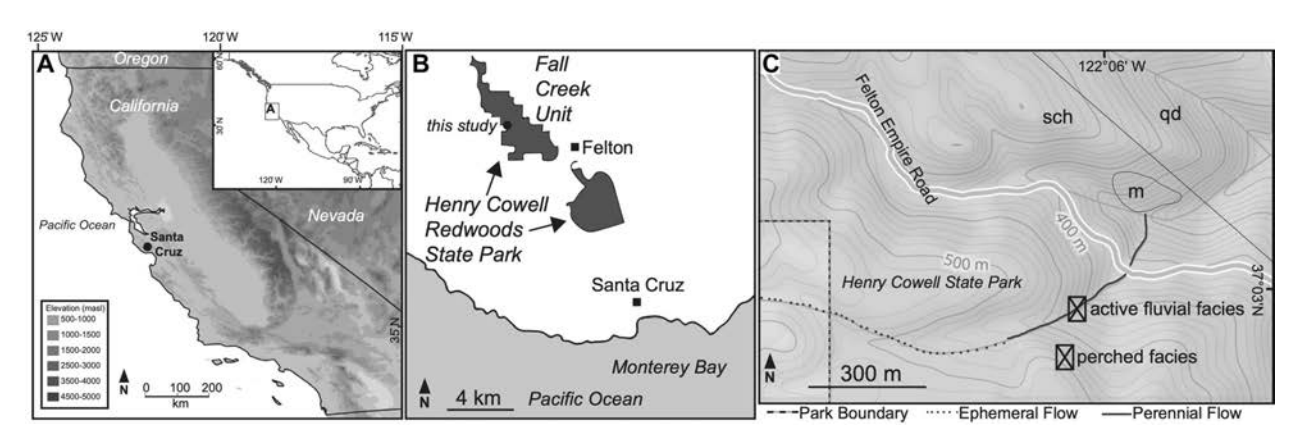


**Figure 1.** (A) Elevation map of California denoting the Santa Cruz area. (B) Regional map of the Santa Cruz area denoting the study site in the Fall Creek Unit of Henry Cowell State Park. (C) Geologic and topographic map showing the active spring fluvial facies and the location of the perched tufa cascade (both marked with an 'X'). Abbreviations: m, marble; sch, metasedimentary rocks mainly pelitic schist and quartzite; qd, quartz diorite, after Clark 1981. Modified after Boelts *et al.*, 2020.

© 2022 John Wiley & Sons, Ltd.

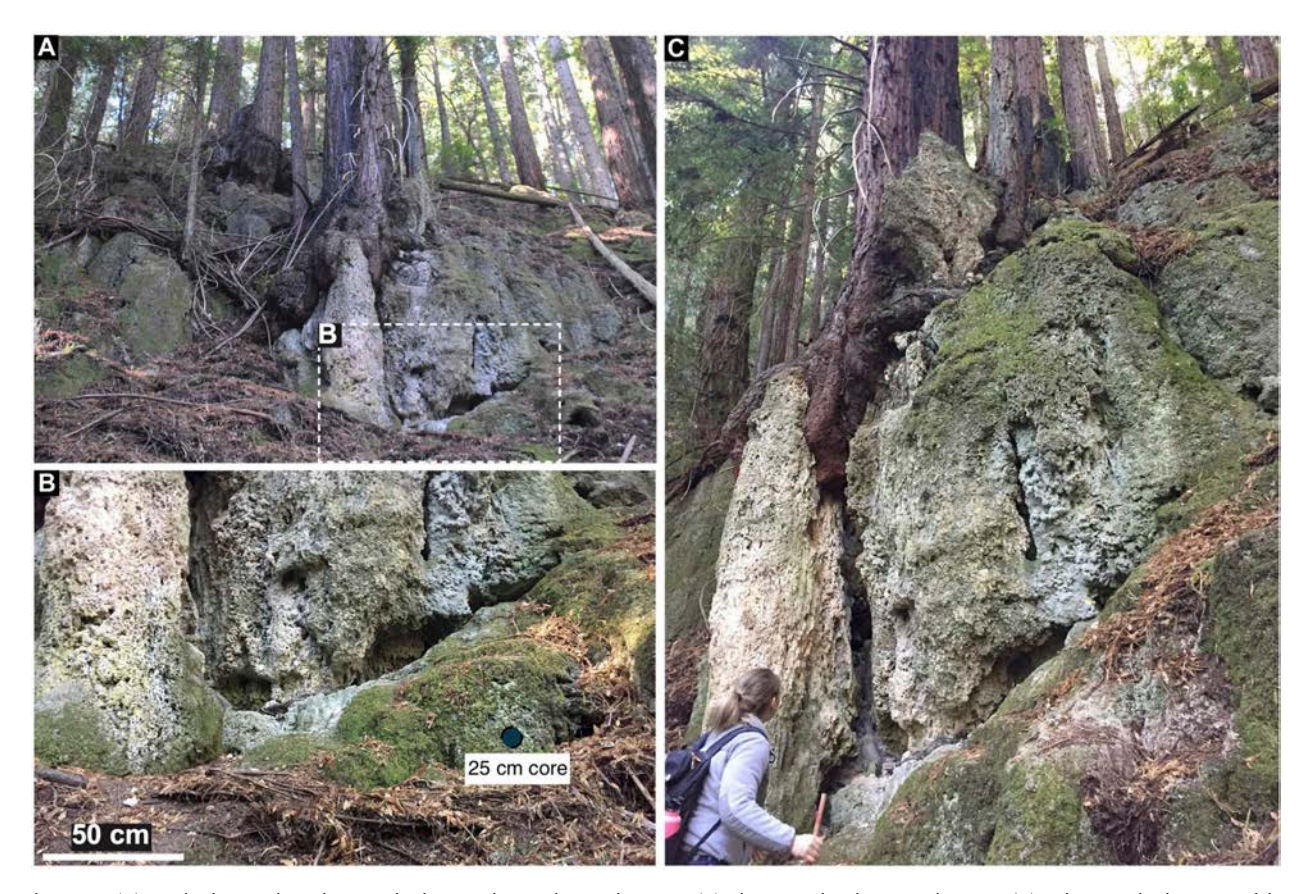


**Figure 2.** (A) Perched cascade carbonates looking in the southwest direction. (B) Close up of carbonates shown in (A) indicating the location of the core sample. Drippy speleothems shown on far left section and tufa curtain in the southern part of the mound. (C) Perched carbonate facies demonstrating progradation towards the valley channel.

collected from the perched site. The three samples were collected *in situ* from the cascade face (Fig. 3A–B).

The core from Henry Cowell (25 cm long and 3 cm in diameter) was extracted horizontally approximately 8 cm from the base of the perched mound, below the tufa curtain (Fig. 2B; Fig. S2). The core was cut in half longitudinally; half was scanned on a flatbed scanner and two samples (each ~5 cm in length) were sent to Global GeoLab Limited for dissolution and extraction of the insoluble residue and preparation of palynological slides. Microscopic fragments of charcoal collected from the insoluble residue of these two samples were dated using radiocarbon (described below).

Six decimetre-scale samples of tufa were collected from the fluvial deposits (Figs 1C and 4). Two samples from the fluvial site originate from the fluvial channel collected *in situ* from the actively-accreting bed and four were collected from float adjacent to the stream channel (Fig. S1). All samples were slabbed and scanned on a high-resolution flatbed scanner. Cross-sections were subsequently converted to petrographic thin sections – nine from the perched mound and five from the fluvial tufa deposits for petrographic analysis.

#### Carbonate isotopic analyses

Carbonate powders from samples of the core from the perched tufa site (n=18) and the fluvial tufa site (n=50) were analysed for stable carbon and oxygen isotopes. Samples were drilled from polished specimens of the perched core, and the fluvial tufa samples. Powders collected from the perched core were drilled along a vertical gradient (Fig. S2) with approximately 0.5 cm between each sample. The lack of banding and

discernible fabric type precluded justifying a more discriminating sampling method.

We targeted calcite laminations in the fluvial samples and note the texture type differentiating between *Oocardium* calcite that is distinguishable at the millimetre scale (Fig. 5G) and calcite spar. Samples labelled with an asterisk in Tables 2 and 3 represent sample averages of at least two sample measurements along the same band. The powdered samples were analysed on a Thermo Fisher Kiel IV-MAT 254 mass spectrometer at the UC Santa Cruz Stable Isotope Laboratory. Carbonate carbon and oxygen isotope ratio data are corrected to % VPDB by two-point correction to NBS18 and CM12 (Carrara Marble calibrated against NBS19). The reproducibility of measurements of standard reference materials was 0.02 % for  $\delta^{13}$ C and 0.12 % for  $\delta^{18}$ O.

#### Radiocarbon analyses

Four accelerator mass spectrometry (AMS) <sup>14</sup>C dates were obtained from organic fragments collected from the ancient tufa mound and modern tufa in Henry Cowell State Park. Two tufa sections of the 25 cm long core from the perched site (the innermost 5 cm and 13–19 cm) contained organics (pollen/charcoal) that underwent <sup>14</sup>C analysis. Charcoal samples were acid-base-treated and then bleached with a 1:1 mixture of 1 N HCl and 1 M NaClO<sub>2</sub> (75°C) prior to combustion and analyses. The associated carbonate from the innermost part of the core was also dated (Fig. 3C). A carbonate sample from the fluvial tufa deposits located adjacent to the current path of the carbonate spring contained large charcoal fragments (Fig. 4D). We hand-picked the largest charcoal piece (measuring ~1 cm²) for <sup>14</sup>C analysis. Samples were sent to the UC Irvine

© 2022 John Wiley & Sons, Ltd.

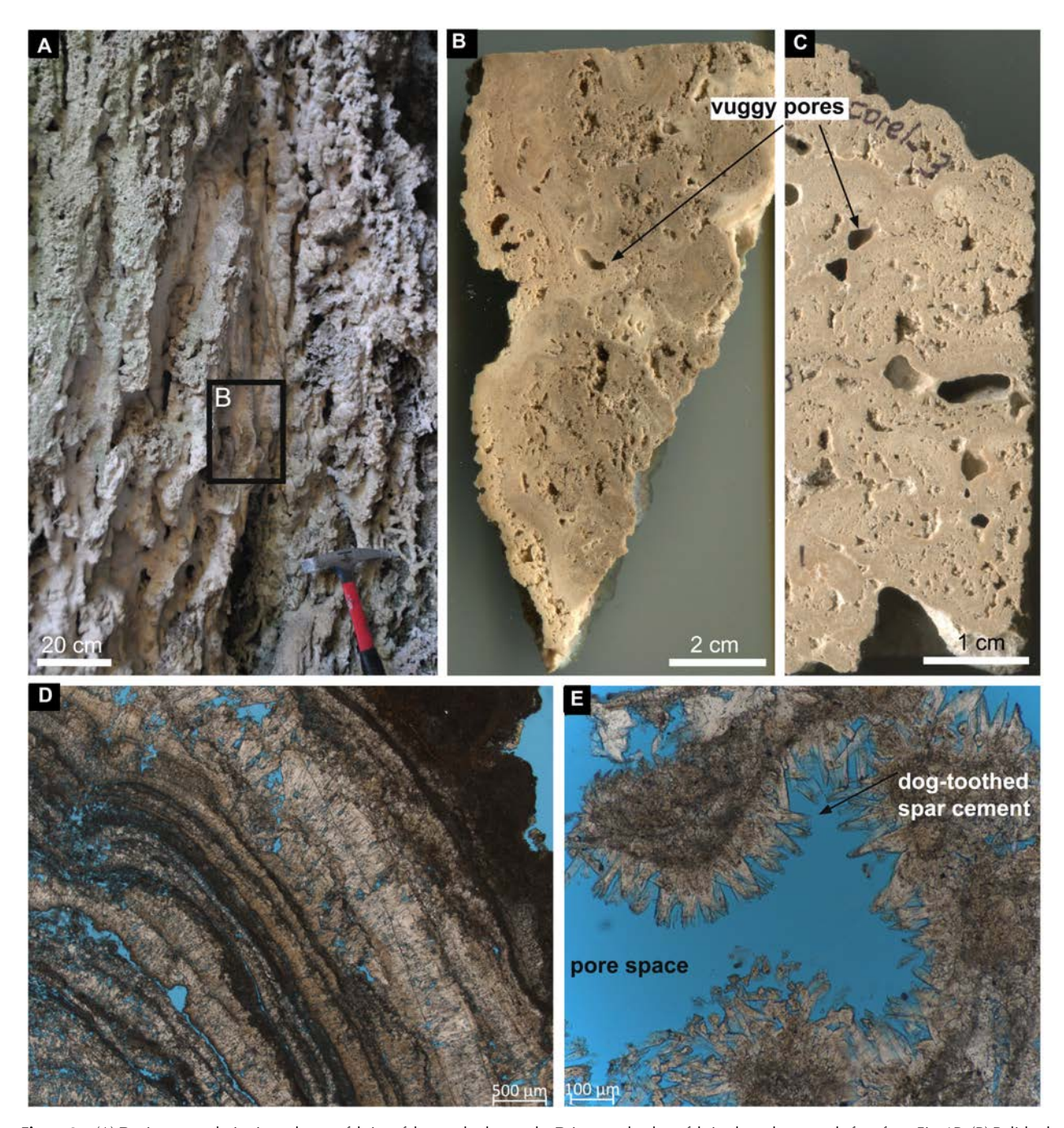


**Figure 3.** (A) Decimetre-scale *in situ* carbonate fabrics of the perched cascade. Drippy speleothem fabric along the cascade face from Fig. 1B. (B) Polished tufa specimen collected from (A). (C) Polished tufa specimen of the core displaying vuggy porosity. (D) Thin section photomicrograph of laminated spar and micrite (dark brown) bands of the cascade tufa. (E) Diagenetic dog-toothed spar cement of the cascade tufa; blue denotes pore space.

Keck Laboratory for radiocarbon analysis. The data were calibrated on CALIB 8.2 (Stuiver *et al.*, 2021) using the calibration curve INTCAL20 for non-marine samples.

#### **Results**

#### Spring carbonate facies

#### Perched carbonates

A polished representative sample of the 25 cm long core is shown in Fig. 3C. The core sample exhibits vuggy porosity and lacks distinct internal lamination (Fig. 3C). Carbonate samples from the perched tufa (Fig. 3A–B) contain irregular banding

at the microscale (Fig. 3D; approximately 0.2–0.5 mm in thickness). The millimetre-scale bands alternate between overlapping sparry and micritic laminae (Fig. 3D). In other parts of the sample, the texture is defined by vuggy, mesoscopic pore space and diagenetic dog-toothed spar cement (Fig. 3E). At a microscopic scale, carbonate fabrics are primarily composed of micrite, microspar and spar – all of which are irregularly distributed.

#### Fluvial carbonates

Adjacent to the perched tufa mound at ~50 m lower elevation in the valley channel, Ringtail Creek hosts actively-accreting fluvial carbonates along its bed. Diatom-rich coated grain

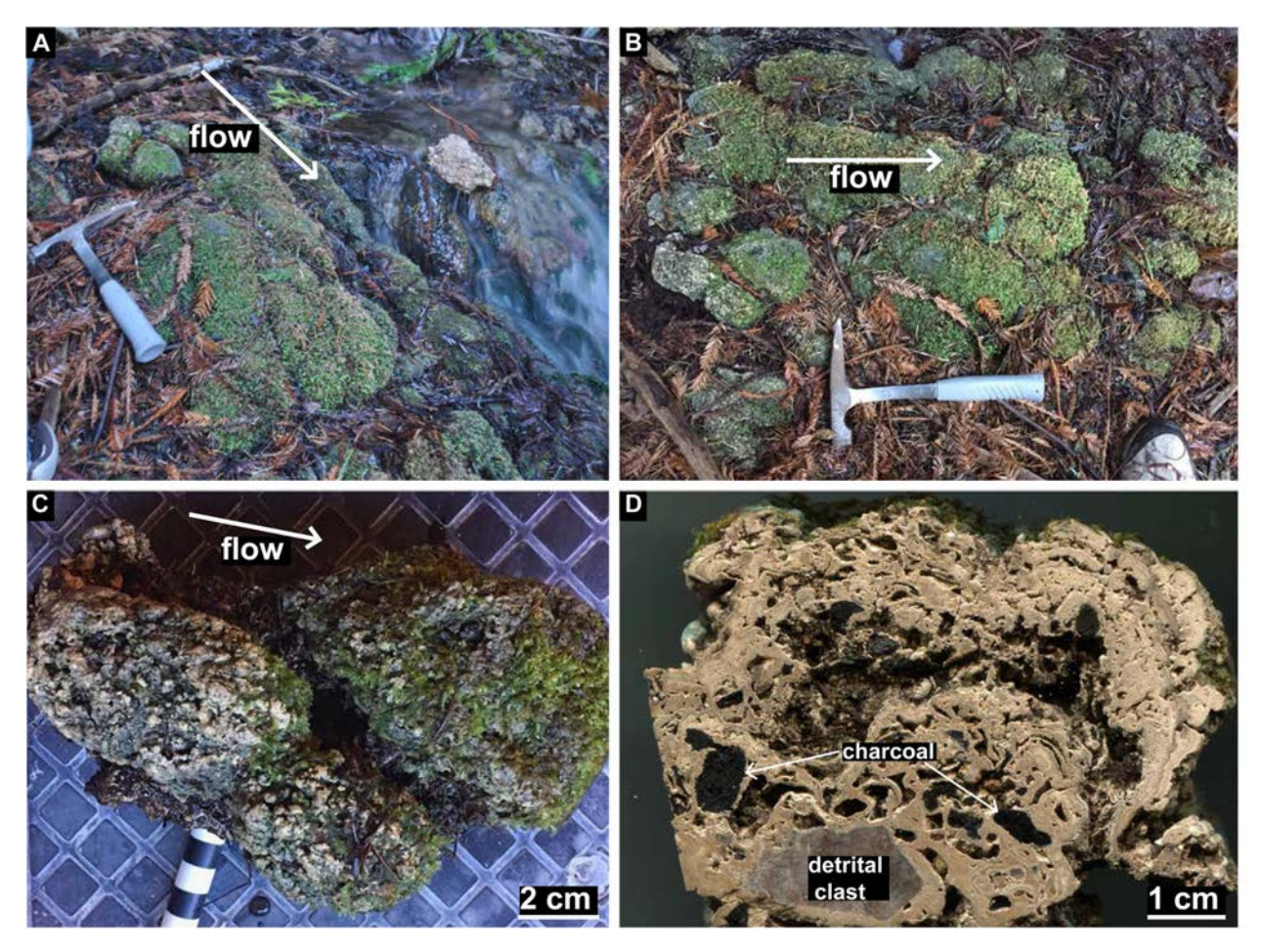


**Figure 4.** (A) Modern spring channel containing recent moss-covered tufa denoting direction of flow. (B) View of (A) from the top denoting flow direction. (C) Distinct centimetre-scale tufa domes (view from the top). (D) Cross-section of one of the centimetre-scale tufa domes from (C) denoting a coarse-grained laminated fabric with charcoal and detrital clast inclusions.

samples from the distalmost spring were described in Boelts et al. (2020). We examined an area spanning approximately 6 m<sup>2</sup> that exhibits paludal/channel and stromatolitic facies (Figs 4-5), located approximately 30 m from the spring source (Fig. 1B). At the macroscale, the carbonates contain decimetrescale domes (Fig. 4). These decimetre-scale domes (Fig. 4B) are laminated and stromatolitic (Fig. 5). The stromatolitic laminations alternate between bands of spar and micrite, but the overall fabric is dominated by alternations of micrite, microspar and spar (Fig. 5B-C). Well-laminated and banded calcite surrounds the inner clastic area, with calcite bands ranging in 0.1–1 mm in thickness. The microtexture ranges from dendritic (Fig. 5D), to densely sparitic (Fig. 5E-F), and exhibits evidence of microbial influence of the carbonate textures in the form of filamentous moulds (Fig. 5E-F), including the calcite microstructure of the freshwater microalgae Oocardium stratum (Fig. 5G) described from other springs in the region (Ibarra and Sanon, 2019). This Oocardium spar fabric (~0.5 cm thick) is discernible on the polished samples (Fig. S1) and was targeted in the isotope analyses as a known biogenic texture (Table 2).

#### Stable isotope results

The carbon and oxygen isotopic values of carbonate powders from the inactive perched tufa and the fluvial tufa deposits from the active stream channel are listed in Tables 2 and 3. The  $\delta^{13}C$  values from the fluvial tufa samples collected near or in the fluvial spring channel range from -10.87% to -8.60%

with a mean value of -10.19  $\pm$  0.45% (1 $\sigma$ , n = 50). The  $\delta^{18}$ O values range from -5.8% to -4.9% with a mean value of -5.4  $\pm$ 0.2‰ (1 $\sigma$ , n = 50). The range in  $\delta^{13}$ C values for the samples from the inactive carbonates (Fig. 2) is -9.65% to -1.76% with a mean value of -8.43  $\pm$  1.73 (1 $\sigma$ , n = 18). The  $\delta^{18}$ O values range from -5.4% to -3.2% with a mean value of -5.0  $\pm$  0.5  $(1\sigma, n = 18)$ . Fig. 6 contains a cross plot of all stable isotope results. The  $\delta^{18} \overset{\smile}{O}$  of the fluvial carbonates are more depleted (t = 4.32, p < 0.001) than the  $\delta^{18}$ O of the perched carbonates. The  $\delta^{13}C$  of the fluvial carbonates are also more depleted (t = 6.59, p < 0.001) than the  $\delta^{13}$ C of the perched carbonates. The samples marked with an asterisk in Tables 2 and 3 represent averages between stable isotopic values of at least two powder samples from the same band where the  $1\sigma$ between replicate samples was 0.14% or better. Stable isotope results of Oocardium calcite laminae of the fluvial tufa deposits are not statistically different from the spar fabrics.

#### Radiocarbon results

The radiocarbon results are listed in Table 4. Charcoal extracted from a piece of carbonate collected near the current fluvial spring flow channel has a calibrated age range of 853  $\pm$  0.4 (2 $\sigma$ ) cal BP. Organic residue (microscopic charcoal fragments) from the perched core have calibrated age ranges of 6.2  $\pm$  0.06 (2 $\sigma$ ) cal ka BP and 8.0  $\pm$  0.04 (2 $\sigma$ ) cal ka BP and corroborate the stratigraphic order we expect given the inferred palaeoflow direction at the time the tufa mound was

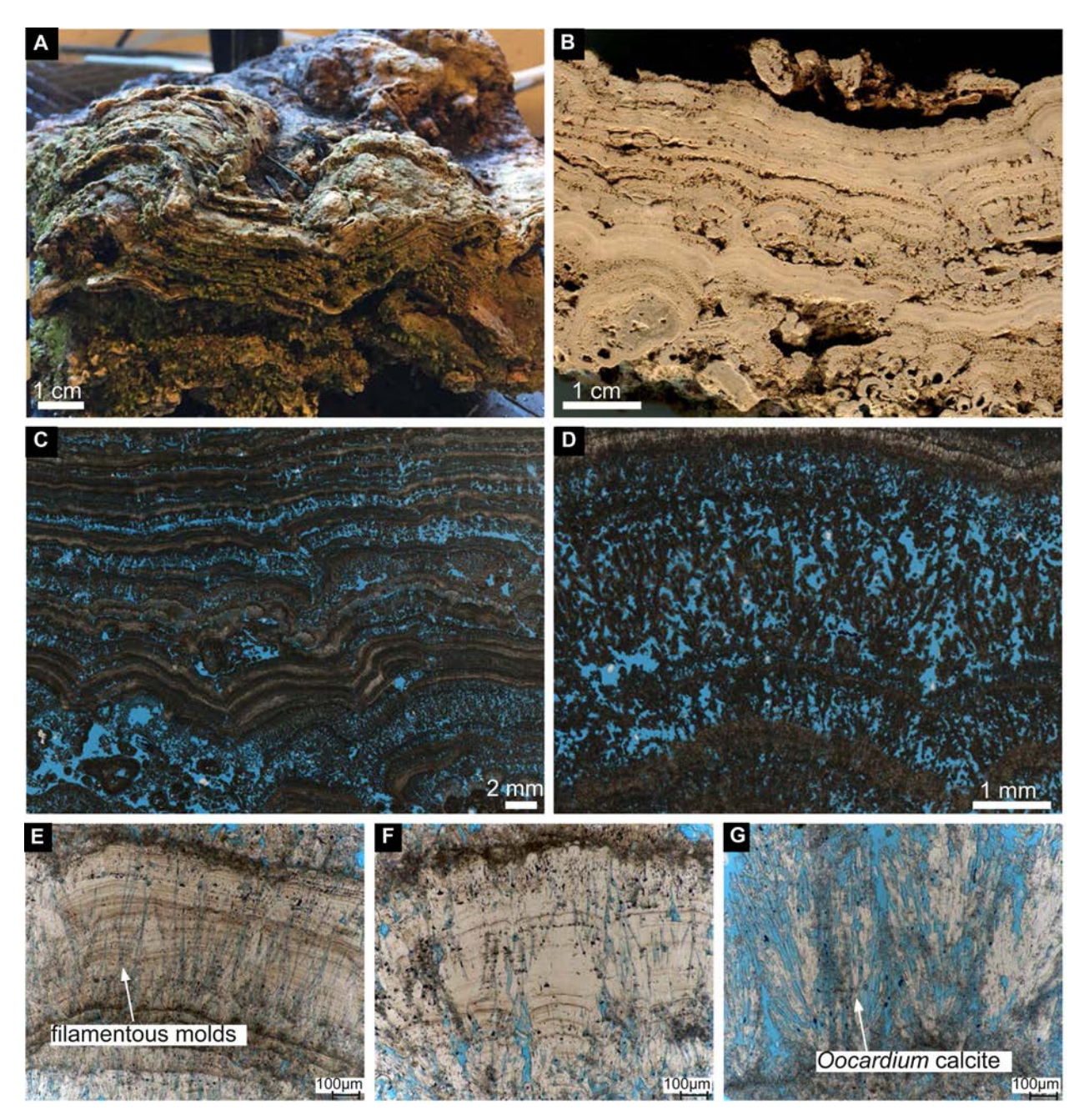


Figure 5. (A) Laminated and stromatolitic tufa from the fluvial spring channel. (B) Polished tufa sample shown in (A) denoting a laterally continuous banded fabric. (C) Thin section photomicrograph of (B) highlighting dendritic and dense spar and micrite laminations. (D) Dendritic calcite from (C). (E–F) Spar calcite crystals containing filamentous moulds. (G) Calcite microstructure of the green alga *Oocardium stratum*. Blue regions signify pore space in all photomicrographs.

deposited. That is, the innermost piece records the older date. The calibrated age of a carbonate sample (HC1-carb) from the core at Henry Cowell State Park is 4030 cy  $_{\rm BP}$ . The  $^{14}C$  age of carbonate, however, likely reflects mixing of soil-derived  $CO_2$  with old bedrock carbon and is therefore not considered meaningful here for temporal reconstruction.

#### **Discussion**

#### Interpretation of facies and stable isotope results

Several lines of evidence (including chronological, geomorphologic, stable isotopic and textural) suggest that the elevated, steep and inactive deposits relative to the active

valley floor fluvial tufa represent different depositional periods. The elevation for the current outflow emergence that feeds Ringtail Creek Spring is 472 m (Table 1), which is ~30 m lower than the elevation of the perched mound (Fig. 1C). This observation suggests the perched tufa formed from either (1) a different adjacent spring whose source has since dried due to a decline in the water table level, (2) the perched deposit formed from an ancient, wetter Ringtail Creek Spring whose outflow channel initiated at an elevation greater than 500 m, thus sustaining growth of the perched tufa, or (3) the perched deposit formed from a spring whose source was cut off or deviated by tectonics during the last ~8 ka.

Consideration of scenario 3 is important given the potential effects of tectonic influence over the last ~8 ka in controlling

**Table 2.** Stable isotopic compositions of  $\delta^{18}O$  and  $\delta^{13}C$  (% VPDB) for carbonates from the perched deposit. Sample ID with core prefix indicate samples from the perched core.

Perched deposit (above valley channel)

Fabric type	Sample ID	δ <sup>13</sup> C (‰ VPDB)	δ <sup>18</sup> Ο (‰ VPDB)	δ <sup>13</sup> C1σ ‰	δ <sup>18</sup> Ο1σ ‰
nd	core1-1-1	-9.2	-4.9		
nd	core1-1-2	-9.3	-5.1		
nd	core1-1-3	-9.15	-5.2		
nd	core1-1-4	-9.34	-4.9		
nd	core1-2-1	-8.62	-5.1		
nd	core1-2-2	-8.36	-5.0		
nd	core1-2-3	-9.48	-5.2		
nd	core1-2-4	-8.81	-5.0		
nd	core1-2-5	-9.16	-5.1		
nd	core1-2-6	-7.97	-5.0		
nd	HC3A-1	-8.07	-5.1		
nd	HC3A-2	-8.59	-4.8		
banded	HC3A-B*	-4.97	-4.3	2.79	0.96
micrite					
nd	core1-3-1	-8.9	-5.3		
nd	core1-3-2	-8.44	-5.3		
nd	core1-3-3	-8.39	-5.2		
nd	core1-3-4	-8.6	-5.3		
nd	core1-3-5	-9.65	-5.4		
	Mean	-8.24	-5.0		
	1σ	1.74	0.47		

<sup>\*</sup>Sample averages of at least two sample measurements along the same band. nd stands for "not discernible."

the depositional base level of the tufa deposits, as the San Andreas Fault zone dominates the structural geology of the study site. However, the outcrop exposures of the large perched facies (Fig. 2) tufa mound do not contain evidence of microfaults or brittle structure deformation that would be indicative of tectonic influence. Instead, the facies represented at the perched mound are typical of cascade facies of tufa curtains (Fig. 2) indicating *in situ* development and thus making scenario 3 less likely or difficult to ascertain.

Scenarios 1 and 2 above suggest that the elevated nature of the perched tufa ~50 m above the valley channel indicates deposition when the water table was higher than its modern level (e.g. Domínguez-Villar et al., 2011). The perched mound is currently located along a steep geomorphic gradient (Fig. 1C) away from the modern spring flow channel, suggesting an ancient spring source or an elevated base level for an ancient Ringtail Creek Spring that once fed the cascade facies (Fig. 2) and sustained an elevated water table during a past pluvial period. A change in hydroclimate from wetter to drier conditions was likely the dominant factor controlling tufa formation at the perched site.

Textural and petrographic differences between the perched tufa (Fig. 2) and the fluvial tufa (Fig. 4) suggest differing exposure times to meteoric conditions. Textures of the tufa samples from the perched site (Fig. 3) contain evidence of meteoric dissolution and diagenetic cementation in the form of vuggy porosity and dog-toothed spar cements (Fig. 3). Such diagenetic textures are typical of the vadose zone and can develop during repeated episodes of cementation and dissolution (e.g. lbarra *et al.*, 2015). The 25 cm core sample is typified by vuggy porosity resulting from meteoric cementation by later fluids (Fig. 3C) which complicated the characterisation of the texture type in the stable isotope samples (Fig. 2). The fluvial tufa deposits contain well-preserved banding (Fig. 5C and

Fig. S1) and evidence of biogenic influence in the form of filamentous moulds on the calcite crystal structures (Fig. 5E–G), indicating depositional or near-depositional conditions reflective of their recent accretion and likely minimal diagenetic alteration. Furthermore, the radiocarbon age of the fluvial tufa charcoal sample provides chronology for recent deposition.

Stable isotope results of carbon and oxygen of the two deposits further corroborate distinct depositional periods. The perched cascade deposits record  $\delta^{13}C$  and  $\delta^{18}O$  values that are more enriched in  $\delta^{13}$ C and  $\delta^{18}$ O (p < 0.001) in comparison with the fluvial carbonates (Fig. 6). The more enriched isotopic values of the perched carbonates can result from evaporative enrichment associated with diagenetic cementation (Andrews, 2006). Alternatively, the observed differences in δ<sup>13</sup>C between the perched and fluvial tufa may be the result of changes in the amount of soil-derived CO2 during a different climatic regime. For example, the more depleted  $\delta^{13}$ C for the fluvial carbonates may reflect a greater incorporation of light soil carbon given the dense vegetation in the valley channel fed by the local spring source. Seasonal changes in soilderived CO<sub>2</sub> can result in  $\delta^{13}$ C variability (Andrews, 2006) and δ<sup>13</sup>C values in freshwater tufa deposits can also be controlled by a combination of water residence time and vegetation density in the catchment (Makhnach et al., 2004). Sampling of known biogenic material of the Oocardium calcite did not reveal a significant difference between biogenic (Oocardium) calcite and spar calcite (Fig. S3). Any small  $\delta^{13}$ C variations are instead likely a result of larger-scale factors such as seasonal changes in water chemistry. Resolving potential differences between biogenic (Oocardium) calcite and other calcite banded textures would require sampling at higher resolution.

The narrow difference in  $\delta^{18}O$  between the perched and fluvial samples are typical of coastal areas where variations in δ<sup>18</sup>O of precipitation are small (Andrews, 2006). Assuming precipitation under equilibrium conditions, which is common from other tufa deposits (Garnett et al., 2004; Andrews et al., 1997; Ibarra et al., 2014),  $\delta^{18} O$  of fluvial tufa is primarily a function of changes in water temperature and the δ<sup>18</sup>O value of the recharging water (Andrews, 2006). In California, the majority of the precipitation moisture is sourced from the Pacific Ocean with north Pacific-sourced moisture characterised by lower  $\delta^{18}O$  values than moisture sourced from tropical storms (Berkelhammer et al., 2012; Wong et al., 2016). Modern average rainfall in Santa Cruz has been measured at -3.03% to -5.37% (Vienna Standard Mean Ocean Water) (Oster et al., 2017). These values are similar to the tufa δ<sup>18</sup>O values recorded in this study (Fig. 6) and corroborate other studies where the  $\delta^{18}\mbox{O}$  of the groundwater is consistent with predictable  $\delta^{18}O$  of the tufa carbonate (Andrews et al., 1993; Arenas et al., 2000; Matsuoka et al., 2001). The ~0.6‰ average enrichment for the perched deposits (Fig. 6) would account for ~1°C change in temperature (Rozanski et al., 1993), which would not be discernible from the expected change in water temperature along the stream gradient (Table 1). It is also important to note other potential effects that may have contributed to the observed early Holocene enrichment in δ<sup>18</sup>O such as rainfall amount effects (Dansgaard, 1964) and moisture condensation height (Buenninget al., 2012). These effects should be considered in future studies where improved chronology can be coupled with higher resolution sampling.

### Comparison with other regional palaeoclimate proxies

Few Quaternary terrestrial records of palaeoclimate are available from the central California coast (Fig. 7 and Table 5).

**Table 3.** Stable isotopic compositions of  $\delta^{18}O$  and  $\delta^{13}C$  (‰ VPDB) for carbonates from the fluvial deposit.

Fluvial carbonates

Fabric type	Sample ID	δ <sup>13</sup> C (‰ VPDB)	δ <sup>18</sup> O (‰ VPDB)	δ <sup>13</sup> C1σ ‰	δ <sup>18</sup> Ο1σ ‰
	- Campie 15	(,00 1.22)	(/// 1.22)	0 0.0 /00	0 0.0 700
spar	T1	-10.73	-5.7		
spar	T2	-10.81	-5.7		
spar	Т3	-10.53	-5.6		
spar	T4	-10.56	-5.6		
spar	F2-F1	-9.9	-5.5		
spar	F2-F2	-9.88	-5.2		
spar	F2-F3	-10.16	-5.4		
spar	F2-F4	-10.23	-5.2		
Ooc. spar	F2-01	-10.31	-5.4		
Ooc. spar	F2-02	-9.99	-5.2		
Ooc. spar	F2-03	-10.39	-5.5		
Ooc. spar	F2-04	-10.31	-5.3		
spar	UHC-4A-F1	-10.68	-5.2		
spar	UHC-4A-F2	-10.57	-5.1		
Ooc. spar	UHC-4A-01	-10.43	-5.2		
Ooc. spar	UHC-4A-02	-10.6	-5.1		
Ooc. spar	UHC-4A-03	-10.8	-5.2		
spar	UHC3A-1	-9.64	-5.3		
spar	UHC3A-2	-9.88	-5.2		
spar	UHC3A-3	-9.78	-5.5		
banded spar	F1	-9.13	-5.4		
banded spar	F2	-9.78	-5.7		
banded spar	F3	-10.37	-5.5		
banded spar	F4*	-10.13	-5.6	0.02	0
banded spar	F5	-8.6	-5.4		_
banded spar	F6	-9.26	-5.2		
banded spar	F7	-10.17	-5.4		
banded spar	F8*	-9.70	-5.3	0.03	0.07
banded spar	F9	-9.97	-5.5	0.03	0.07
banded spar	F10	-10.87	-5.4		
banded spar	F11	-10.46	-5.4		
banded spar	F12*	-10.11	-5.5	0.03	0.14
banded spar	F13*	-10.11	-5.5 -5.5	0.03	0
banded spar	F14*	-10.77	−5. <i>7</i>	0.01	0.06
spar	HC1-C-D1	-10.77	-4.9	0.01	0.00
spar	HC1-C-D1	-10.69	-5.3		
•	HC1-C-D3	-10.47	-5.2		
spar	HC1-C-D3	-10.47 -10.13	-3.2 -4.9		
spar	HC1-C-D5	-10.13 -10.52	-4.9 -5.1		
spar	HC1-C-D3	-10.32 -10.47	-5.5		
Ooc. spar	HC1-C-01	-10.47 -10.2	-5.5 -5.4		
			-5.4 -5.4		
Ooc. spar	HC1-C-03	-10.24			
Ooc. spar	HC1-C-04	-10.4	-5.3 5.3		
Ooc. spar	HC1-C-05	-9.83	-5.2 5.3		
Ooc. spar	HC1-C-06	-10.28	-5.2 5.36		
	Mean	-10.19	-5.36		
	1σ	0.45	0.21		

<sup>\*</sup>Sample averages of at least two sample measurements along the same band. Ooc. samples correspond to the fabric of *Oocardium stratum* (Fig. 5G).

Arguably the most robust terrestrial proxy of palaeoclimate in the region is the pollen record (Rypins *et al.*, 1989, Adam *et al.*, 1981). Rypins *et al.*, (1989) analysed pollen from Point Reyes, CA (210 km north of Santa Cruz) to model past shifts in plant ecology. Between 12 ka and 10 ka, the area was dominated by *Abies* (fir) and *Pseudotsuga* (Douglas fir), implying cooler and wetter conditions. Adam *et al.* (1981) analysed pollen and <sup>14</sup>C of plant debris from Clear Lake, CA (280 km north of Santa Cruz), where their results indicate a transition from cooler and wetter conditions to warmer, modern-day climate between 15 ka and 10.4 ka inferred from a gradual increase in *Quercus* (oak) and decrease in *Pinus* (pine) during that time period. The difference in timing between Rypins *et al.* (1989) and Adam *et al.* (1981) could

be attributed to the differing climates between Point Reyes, CA and Clear Lake, CA – where Point Reyes is coastal and experiences relatively cooler summers than Clear Lake, which is further inland (Fig. 7). Reneau *et al.* (1986) analysed <sup>14</sup>C of charcoal from basal colluvium in hollows in Marin County, CA (130 km north of Santa Cruz) to model past landslide events. Such erosional events are thought to be climatically controlled and/or attributed to changes in vegetation. Thus, Reneau *et al.* (1986) attribute an increase in the frequency of landslides between 11 ka and 9 ka to indicate heavier rainfall. The most proximal terrestrial record to our site is that of a speleothem (stalagmite) from White Moon Cave, near Davenport, CA (Oster *et al.*, 2017). The White Moon Cave record indicates that coastal California experienced an increase in effective

moisture at 8.2 ka. The White Moon Cave speleothem study also records the first semi-quantitative hydroclimate record that goes beyond the tree ring record (de Wet et~al.,~2021) by reconstructing precipitation change during the early Holocene using calcium isotopes of calcite stalagmite. The  $8.0\pm0.04~(2\sigma)$  cal ka BP wet event recorded in the perched tufa in this study corroborates coincident growth episodes that indicate wetter conditions from two independent proxies (fluvial tufa and speleothems) from the same region.

Marine sediments off the central California coast also include pollen data from deep-sea cores at ODP site 1018 (75 km west of Santa Cruz, CA) (Lyle *et al.*, 2010; Fig. 7,

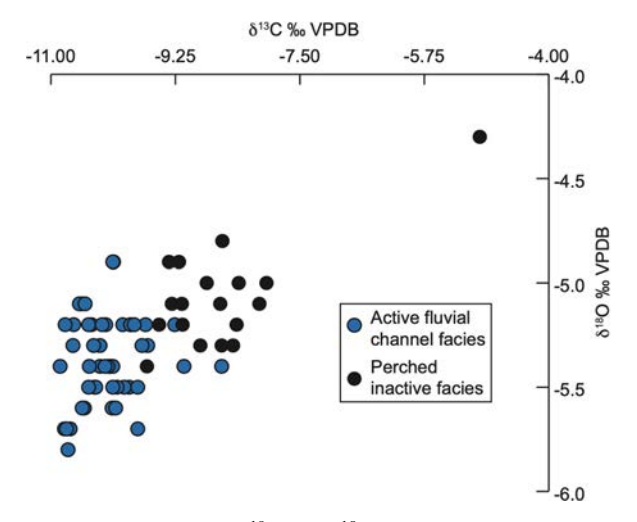


Figure 6. Cross plot of  $\delta^{13}C$  and  $\delta^{18}O$  of carbonate tufa from the perched and fluvial tufa samples.

Table 3). Palynology analyses reveal a relatively low abundance of herbs, grasses and shrubs with a high abundance of forest communities (alder, oak and redwood) from 13 ka to 5 ka, signalling wetter conditions and corroborating the episodes of tufa deposition in this study. Additional palynology analyses from a core located approximately 100 km west of the mouth of the Russian River (VI-80-P3) shows that *Alnus* (alders) increase in abundance at around 16 ka and decline at 7 ka (Gardner *et al.*, 1988). The presence of alders favours colder and wetter climates. Findings from Gardner *et al.* (1988) place the climate in 'disequilibrium' from 15 ka to 5 ka, and a wet event could have occurred within that time frame as is supported by the pollen data.

Although these studies, and others (e.g. Lyle et al., 2001; Heusser and Shackleton, 1979), have found correlations between onshore and offshore climate, none of the proxies summarised in Table 3 (with the exception of the White Moon Cave record) are a direct indication of increased rainfall or elevated water tables, making the tufas in the Santa Cruz region, and karst geology in general, a particularly valuable addition to the region's palaeoclimate record. All of the records mentioned, however, indicate the same broad trend: a wetter and colder climate during the Pleistocene through the Pleistocene-Holocene transition and then long-term drying conditions up to today. The tufa ages support higher groundwater discharge and therefore heavier rainfall (i.e. a pluvial) during the early to mid-Holocene (~6-8 ka), thus generally agreeing with other regional proxies of palaeoclimate. The ages of the tufa correspond most closely to the terrestrial records mentioned above, which may reflect the differing sensitivities between proxies and depositional settings. Together, geomorphologic, petrographic, radiometric and stable

**Table 4.** <sup>14</sup>C age data for carbonate and organics from the tufa deposits.

UCIAMS	Sample name	Location	<sup>14</sup> С age (вр)	±	2 sigma range <sup>a</sup>	Age Су вр <sup>а</sup>
240214	UHC1-charco	al Henry Cowell Fluvial	920	20	840–911	853
240216	HC3-residue	Henry Cowell Perched	5380	20	6227-6279	6206
240217	HC1-residue	Henry Cowell Perched	7170	20	7944-8017	7986
240222	HC1-carb	Henry Cowell Perched	3675	20	3963-4088	4030

<sup>&</sup>lt;sup>a</sup>Calibrated age on IntCAL Reimer et al., 2020.

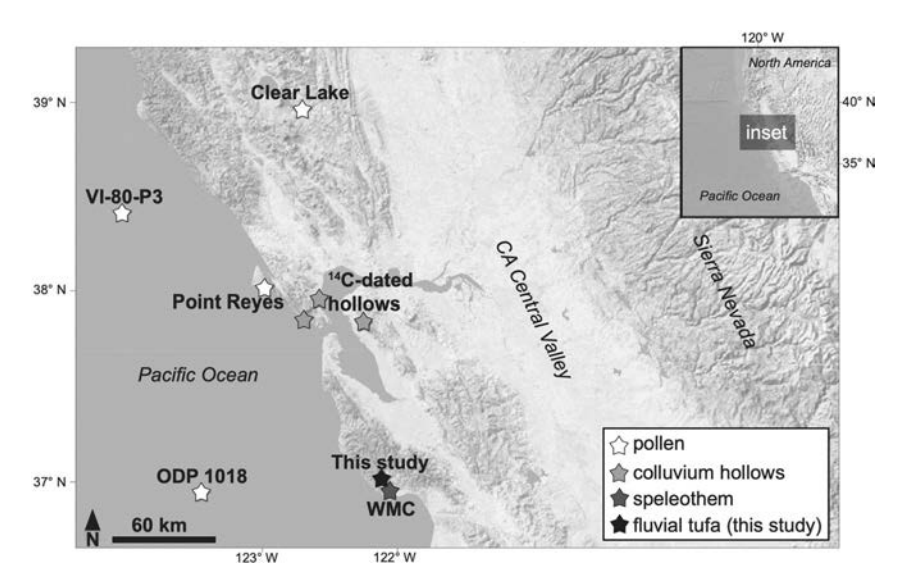


**Figure 7.** Regional map of coastal central California indicating the proximal climate records discussed in the text.

© 2022 John Wiley & Sons, Ltd. J. Quaternary Sci., 1–12 (2022)

Table 5. Timing of coastal central California Holocene wet events.

Reference	Proxy	Timing of wet event
Lyle <i>et al.</i> , 2010	Pollen and benthic foraminifera stable oxygen isotopes	13 ka to 5 ka
Reneau et al., 1986	<sup>14</sup> C of charcoal from basal colluvium in 11 California hollows	15 ka to 9 ka
Oster et al., 2017	Carbon and oxygen isotope analysis and U-series dating of stalagmite cores; Ca isotopes	8.6 ka to 6.9 ka
de Wet <i>et al.,</i> 2021		
Rypins et al., 1989	Pollen and <sup>14</sup> C	12 ka to 9.4 ka
Adam <i>et al.,</i> 1981	Pollen and <sup>14</sup> C	15 ka to 10.4 ka
Gardner et al., 1988	Pollen	16 ka to 7 ka

isotopic differences between the cascade facies (Fig. 2) and the fluvial carbonates (Fig. 4) indicate strong evidence of a past pluvial period that controlled tufa formation at a higher elevation than modern spring flow. Importantly, the ages presented here represent a minimum age of ~8 ka, as there is likely additional older tufa that was not sampled or may have since eroded from the steep outcrop face, due to their high relief.

It is also important to note the abundance of charcoal in the core and at this site in general. Wildfires are common in California (Goss *et al.*, 2020) and notably, this site burned during the course of this investigation in the 2020 CZU Lighting Complex Fire. The charcoal fragments and any future studies on the charcoal from this site would provide an important perspective on future changes in extreme climate events. Importantly, the evidence of wildfire in a deposit that represents deposition at a time of an elevated water table may seem contradictory; however, we do not capture sufficient temporal resolution to address the timing and frequency of wildfires in the region.

#### **Conclusions**

Spring-associated fluvial tufa deposits from Henry Cowell State Park, CA, are a valuable moisture-sensitive proxy and addition to the Quaternary palaeohydroclimate record of the region. The ages of the ancient tufa Henry Cowell State Park - from <sup>14</sup>C - corroborate other regional records of palaeoclimate and support wetter conditions (i.e. pluvials) during the early to middle Holocene (~6-8 ka). The differences between the perched and fluvial carbonates indicate two distinct depositional settings; the perched carbonates likely formed in a wetter climate and the fluvial carbonates formed in relatively drier conditions. Depositional ages agree with the timing of other regional proxies that reveal colder and wetter conditions in the early to mid-Holocene. 14C analysis of charcoal from the fluvial carbonates shows that they formed relatively more recently (~850 years BP) and likely under present-day conditions. These moisture-sensitive terrestrial proxies provide valuable complementary insight to high-resolution local palaeoclimate proxies to better reconstruct Holocene hydroclimates from areas that are prone to drought. (Table 5)

Acknowledgements. We thank the California State Park's Santa Cruz District for access to the research site. L. Cortes was supported by an NSF REU grant (EAR-1852564). E. Beverly, A. Erhardt and an anonymous reviewer provided valuable feedback that helped improve the manuscript. Special thanks to the UC Santa Cruz Stable Isotope Laboratory for carrying out the stable isotope analyses and the UC Irvine Keck Laboratory for the radiocarbon analyses. This work was conducted on the land of the Awaswas-speaking people of the Ohlone tribe in Santa Cruz, CA (Aulinta). We have no conflicts of interest to declare.

#### **Supporting information**

Additional supporting information can be found in the online version of this article.

#### References

Adam DP, Sims JD, Throckmorton CK. 1981. 130,000-yr continuous pollen record from Clear Lake, Lake County, California. *Geology* 9: 373–377.

Andrews JE. 2006. Palaeoclimatic records from stable isotopes in riverine tufas: Synthesis and review. *Earth-Science Reviews* **75**: 85–104.

Andrews JE, Brasier AT. 2005. Seasonal records of climatic change in annually laminated tufas: Short review and future prospects. *Journal of Quaternary Science* **20**: 411–421.

Andrews JE, Riding R, Dennis PF. 1993. Stable isotopic compositions of Recent freshwater cyanobacterial carbonates from the British Isles: local and regional environmental controls. *Sedimentology* **40**: 303–314.

Andrews JE, Riding R, Dennis PF. 1997. The stable isotope record of environmental and climatic signals in modern terrestrial microbial carbonates from. *Europe Paleogeography, Palaeoclimatology, Paleoecology* **129**: 171–189.

Andrews JE, Pedley M, Dennis PF. 2000. Palaeoenvironmental records in Holocene Spanish tufas: A stable isotope approach in search of reliable climatic archives. *Sedimentology* **47**: 961–978.

Arenas C, Jones B. 2017. Temporal and environmental significance of microbial lamination: Insights from Recent fluvial stromatolites in the River Piedra, Spain. *Sedimentology* **64**: 1597–1629.

Arenas C, Gutiérrez F, Osácar C et al. 2000. Sedimentology and geochemistry of fluvio-lacustrine tufa deposits controlled by evaporite solution subsidence in the central Ebro Depression, NE Spain. Sedimentology 47: 883–909.

Arp G, Wedemeyer N, Reitner J. 2001. Fluvial tufa formation in a hard-water creek (Deinschwanger Bach, Franconian Alb, Germany). Facies 37: 1–22.

Arenas C, Vázquez-Urbez M, Auqué L *et al.* 2014a. Intrinsic and extrinsic controls of spatial and temporal variations in modern fluvial tufa sedimentation: A thirteen-year record from a semi-arid environment. *Sedimentology* **61**: 90–132.

Arenas C, Vázquez-Urbez M, Pardo G et al. 2014b. Sedimentology and depositional architecture of tufas deposited in stepped fluvial systems of changing slope: Lessons from the quaternary añamaza valley (Iberian Range, Spain). Sedimentology 61: 133–171.

Berkelhammer M, Stott L, Yoshimura K *et al.* 2012. Synoptic and mesoscale controls on the isotopic composition of precipitation in the western United States. *Climate Dynamics* **38**: 433–454.

Beverly EJ, Driese SG, Peppe DJ *et al.* 2015. Recurrent spring-fed rivers in a Middle to Late Pleistocene semi-arid grassland: Implications for environments of early humans in the Lake Victoria Basin, Kenya. *Sedimentology* **62**: 1611–1635.

Boelts H, Ibarra Y, Hayzelden C. 2020. Investigating the Influence of Diatoms on the Textures of Coated Grains From a Carbonate Spring in Northern California. *Journal of Sedimentary Research* **90**: 1601–1613.

Brabb EE. 1989. Studies in Tertiary stratigraphy of the California Coast Ranges *US Geological Survey Professional Paper* **1213**.

Buenning NH, Stott L, Yoshimura K *et al.* 2012. The cause of the seasonal variation in the oxygen isotopic composition of precipitation along the western U.S. coast. *Journal of Geophysical Research Atmospheres* **117**: D18114.

- California State Parks. 2011. Henry Cowell Redwoods State Park [web page]. Available from: https://www.parks.ca.gov/pages/546/files/HenryCowellRedwoodsFinalWebLayout080117.pdf.
- Capezzuoli E, Gandin A, Pedley M. 2014. Decoding tufa and travertine (freshwater carbonates) in the sedimentary record: The state of the art. *Sedimentology* **61**: 1–21.
- Clark J. 1981. Stratigraphy, paleontology, and geology of the central Santa Cruz Mountains, California Coast Ranges. Professional Paper 1168: US Department of the Interior, Geological Survey.
- Cook E, Seager R, Heim RR *et al.* 2010. Megadroughts in North America: placing IPCC projections of hydroclimate change in a long-term paleoclimate context. *Journal of Quaternary Science* **25**: 48–61.
- Cook BI, Ault TR, Smerdon JE. 2015. Unprecedented 21st century drought risk in the American Southwest and Central Plains. Science Advances 1: 1–7.
- Cremaschi M, Zerboni A, Spötl C et al. 2010. The calcareous tufa in the Tadrart Acacus Mt. (SW Fezzan, Libya). An early Holocene palaeoclimate archive in the central Sahara. *Palaeogeography, Palaeoclimatology, Palaeoecology* **287**: 81–94.
- Dansgaard W. 1964. Stable isotopes in precipitation. *Tellus* **16**: 436–468.
- Desouky HE, Soete J, Claes H *et al.* 2015. Novel applications of fluid inclusions and isotope geochemistry in unravelling the genesis of fossil travertine systems. *Sedimentology* **62**: 27–56.
- de Wet CB, Erhardt AM, Sharp WD *et al.* 2021. Semiquantitative Estimates of Rainfall Variability During the 8.2 kyr Event in California Using Speleothem Calcium Isotope Ratios. *Geophysical Research Letters* **48**: 1–11.
- Domínguez-Villar D, Vázquez-Navarro JA, Cheng H *et al.* 2011. Freshwater tufa record from Spain supports evidence for the past interglacial being wetter than the Holocene in the Mediterranean region. *Global and Planetary Change* **77**: 129–141.
- Ford TD, Pedley HM. 1996. A review of tufa and travertine deposits of the world. *Earth-Science Reviews* **41**: 117–175.
- Gardner JV, Park M, Heusser LE *et al.* 1988. Clear Lake record vs. the adjacent marine record; A correlation of their past 20,000 years of paleoclimatic and paleoceanographic responses. *Geologic Society of America* **214**: 171–182.
- Garnett ER, Andrews JE, Preece RC *et al.* 2004. Climatic change recorded by stable isotopes and trace elements in a British Holocene tufa. *Journal of Quaternary Science* **19**: 251–262.
- Goss M, Swain DL, Abatzoglou JT et al. 2020. Climate change is increasing the likelihood of extreme autumn wildfire conditions across California. Environmental Research Letters 15: 094016.
- Heusser LE, Shackleton NJ. 1979. Direct Marine-Continental Correlation: 150,000-Year Oxygen Isotope-Pollen Record from the North Pacific. *Science* **204**: 837–839.
- Ibarra Y, Sanon S. 2019. A freshwater analog for the production of Epiphyton-like microfossils. Geobiology 17: 510–522.
- Ibarra Y, Corsetti FA, Cheetham MI et al. 2014. Were fossil springassociated carbonates near Zaca Lake, Santa Barbara, California deposited under an ambient or thermal regime? Sedimentary Geology 301: 15–25.
- Ibarra Y, Corsetti FA, Feakins SJ et al. 2015. Fluvial tufa evidence of Late Pleistocene wet intervals from Santa Barbara, California, U.S.A. Palaeogeography, Palaeoclimatology, Palaeoecology 422: 36–45.
- Jasechko S, Perrone D. 2021. Global groundwater wells at risk of running dry. Science 372: 418–421.
- Kano A, Matsuoka J, Kojo T *et al.* 2003. Origin of annual laminations in tufa deposits, southwest Japan. *Palaeogeography, Palaeoclimatology, Palaeoecology* **191**: 243–262.
- Knott JR, Machette MN, Wan E et al. 2018. Late Neogene Quaternary tephrochronology, stratigraphy, and paleoclimate of Death Valley, California, USA. *GSA Bulletin* **130**: 1231–1255.
- Lyle M, Heusser L, Herbert T *et al.* 2001. Interglacial theme and variations: 500 k.y. of orbital forcing and associated responses from the terrestrial and marine biosphere, U.S. Pacific Northwest. *Geology* **29**: 1115–1118.
- Lyle M, Heusser L, Ravelo C *et al.* 2010. Pleistocene water cycle and eastern boundary current processes along the California continental margin. *Paleoceanography* **25**: 1–19.

- Makhnach N, Zernitskaja V, Kolosov I *et al.* 2004. Stable oxygen and carbon isotopes in Late Glacial-Holocene freshwater carbonates from Belarus and their palaeoclimatic implications. *Palaeogeography, Palaeoclimatology, Palaeoecology* **209**: 73–101.
- Matsuoka J, Kano A, Oba T *et al.* 2001. Seasonal variation of stable isotopic compositions recorded in a laminated tufa, SW Japan. *Earth and Planetary Science Letters* **192**: 31–44.
- Oster JL, Sharp W, Covey A *et al.* 2017. Climate responses to the 8.2 ka event in coastal California. *Scientific Reports* 7: 1–9.
- Özkul M, Kele S, Gökgöz A *et al.* 2013. Comparison of the Quaternary travertine sites in the Denizli extensional basin based on their depositional and geochemical data. *Sedimentary Geology* **294**: 179–204.
- Pedley M. 2009. Tufas and travertines of the Mediterranean region: A testing ground for freshwater carbonate concepts and developments. *Sedimentology* **56**: 221–246.
- Pedley M, González Martín JA, Ordónez, Delgado S et al. 2003. Sedimentology of quaternary perched springline and paludal tufas: Criteria for recognition, with examples from Guadalajara Province, Spain. Sedimentology **50**: 23–44.
- Reimer PJ, Austin W, Bard E et al. 2020. The IntCal20 Northern Hemisphere. Radiocarbon Age Calibration Curve (0-55 cal kBP) Radiocarbon 62: 725–757.
- Reneau SL, Dietrich WE, Dorn RI *et al.* 1986. Geomorphic and paleoclimatic implications of latest Pleistocene radiocarbon dates from colluvium-mantled hollows, California. *Geology* **14**: 655–658.
- Rodríguez-Berriguete Á, Alonso-Zarza AM. 2019. Controlling factors and implications for travertine and tufa deposition in a volcanic setting. *Sedimentary Geology* **381**: 13–28.
- Rozanski K, Araguas-Araguas L, Gonfiantini R. 1993. Isotopic patterns in modern global precipitation. In *Climate Change in Continental Isotope Records,* Swart PK (ed). American Geophysical Union Monographs, 1–36.
- Rypins S, Reneau SL, Byrne R *et al.* 1989. Palynologic and geomorphic evidence for environmental change during the Pleistocene-Holocene transition at Point Reyes Peninsula, central coastal California. *Quaternary Research* **32**: 72–87.
- Sancho C, Arenas C, Vázquez-Urbez M et al. 2015. Climatic implications of the Quaternary fluvial tufa record in the NE lberian Peninsula over the last 500ka. *Quaternary Research* 84: 398–414
- Sanders D, Wertl W, Rott E. 2010. Spring-associated limestones of the Eastern Alps: Overview of facies, deposystems, minerals, and biota. *Facies* **57**: 395–416.
- Seager R, Neelin D, Simpson I *et al.* 2014. Dynamical and thermodynamical causes of large-scale changes in the hydrological cycle over North America in response to global warming. *Journal of Climate* 27: 7921–7948.
- Shiraishi F, Reimer A, Bissett A *et al.* 2008. Microbial effects on biofilm calcification, ambient water chemistry and stable isotope records in a highly supersaturated setting (Westerhöfer Bach, Germany). *Palaeogeography, Palaeoclimatology, Palaeoecology* **262:** 91–106.
- Shiraishi F, Okumura T, Takahashi Y *et al.* 2010. Influence of microbial photosynthesis on tufa stromatolite formation and ambient water chemistry, SW Japan. *Geochimica et Cosmochimica Acta* **74**: 5289–5304.
- Spiro B, Pentecost A. 1991. One day in the life of a stream—a diurnal inorganic carbon mass balance for a travertine-depositing stream (Waterfall Beck, Yorkshire). *Geomicrobiology Journal* 9: 1–11.
- Springer KB, Manker CR, Pigati JS. 2015. Dynamic response of desert wetlands to abrupt climate change. *Proceedings of the National Academy of Sciences of the United States of America* **112**: 14522–14526.
- Stuiver M, Reimer PJ, Reimer RW. 2021. CALIB 8.2 [online program] at http://calib.org, accessed 10 May 2021.
- Swain DL, Langenbrunner B, Neelin JD et al. 2018. Increasing precipitation volatility in twenty-first-century California. Nature Climate Change 8: 427–433.
- U.S. Department of Commerce, National Climatic Data Center. 2022. National Oceanic & Atmospheric Administration home page

- [web page] Available at http://www.ncdc.noaa.gov/cdo-web/search?datasetid=ANNUAL, accessed 19 May 2022.
- Viles HA, Taylor MP, Nicoll K *et al.* 2007. Facies evidence of hydroclimatic regime shifts in tufa depositional sequences from the arid Naukluft Mountains, Namibia. *Sedimentary Geology* **195**: 39–53.
- Wong Cl, Potter GL, Montañez IP *et al.* 2016. Evolution of moisture transport to the western U.S. during the last deglaciation. *Geophysical Research Letters* **43**: 3468–3477.
- Yao J, Liu H, Huang J *et al.* 2020. Accelerated dryland expansion regulates future variability in dryland gross primary production. *Nature Communications* **11**: 1665.